THE AMERICAN MINERALOGIST, VOL. 55, SEPTEMBER-OCTOBER, 1970

MINERALOGICAL STUDIES OF THE NITRATE DEPOSITS OF CHILE. II. DARAPSKITE, $Na_3(NO_3)(SO_4)\cdot H_2O$[1]

GEORGE E. ERICKSEN AND MARY E. MROSE, *U.S. Geological Survey, Washington, D.C. 20242.*

ABSTRACT

Darapskite, $Na_3(NO_3)(SO_4)\cdot H_2O$, though occurring only sparsely at four other localities, is widespread in the nitrate deposits of Chile. It occurs as euhedral crystals in cavities and as platy to granular material admixed with other saline minerals. The abundance of darapskite here and its scarcity elsewhere results from the exceptionally high concentration of nitrate in the deposits and can be explained by the phase relations in the system $NaNO_3$–$NaCl$–Na_2SO_4–H_2O, which includes the principal saline components of the nitrate ore.

Crystals from Oficina Alemania are monoclinic, $P2_1/m$; $a=10.564\pm0.002$ Å, $b=6.913\pm0.001$ Å, $c=5.1890\pm0.0009$ Å, $\beta=102°\ 47.8'\pm0.8'$, $Z=2$, ρ(meas) 2.202 g/cm³. X-ray powder diffraction data for darapskite, presented for the first time, show the following strong lines: 10.29 Å (100) (100); 3.456 Å (35) (020); 2.865 Å (35) (220) and (021); 2.594 Å (30) ($\bar{1}02$); 4.13 Å (25) (210); and 3.522 Å (25) ($\bar{2}11$). The line $d=10.29$ Å is extremely sensitive and appears in mixtures of saline minerals that contain as little as ⅓ of a percent darapskite. Comparison of physical, optical, crystallographic, and X-ray data confirms published data and demonstrates very close similarity between natural and synthetic darapskite.

INTRODUCTION

This paper is the second of a series of reports describing the physical, chemical, optical, and crystallographic properties, and the distribution and abundance of the saline minerals found in the nitrate deposits of Chile. The first paper (Mrose and Ericksen, 1970) was an outgrowth of the study of darapskite; it shows that the so-called mineral nitroglauberite is darapskite. In addition to the discussion of darapskite, the nitrate deposits are briefly described as a background for discussion of mineralogy in this and later papers. The mineralogical studies are part of a broad geological investigation that is aimed at determining the origin of these unique deposits. The work is being carried out in cooperation with the Instituto de Investigaciones Geológicas of Chile.

Darapskite, $Na_3(NO_3)(SO_4)\cdot H_2O$, first described by Dietze (1891) and named for Luis Darapsky of Santiago, Chile, is a widespread mineral in the Chilean nitrate deposits. Only four other occurrences of darapskite are known: 1) in the Chuquicamata copper deposit (Chile) where it occurs in veins, as much as 6 inches wide (Jarrell, 1939, p. 634–635), associated with the following minerals: kroehnkite, $Na_2Cu(SO_4)_2\cdot 2H_2O$; bloedite, $Na_2Mg(SO_4)_2\cdot 4H_2O$; mirabilite, $Na_2SO_4\cdot 10H_2O$; and epso-

[1] Publication authorized by the Director, U. S. Geological Survey.

mite, $MgSO_4 \cdot 7H_2O$; 2) in the nitrate deposits of Death Valley, California, where it is associated with soda-niter, $NaNO_3$, and niter, KNO_3 (Palache *et al.*, 1951, p. 310); 3) in saline material from caves in limestone, Funeral Mountains (not previously reported; identified by Mrose in material collected by James McAllister of the U. S. Geological Survey, 1965); and supposedly 4) in saline arid soil on the Roberts Massif, Shackleton Glacier, Antarctica (Claridge and Campbell, 1968). Osann (1894) reported on the morphology of darapskite from Oficina[1] Lautaro, which is between Oficina Flor de Chile and Oficina Alemania (Fig. 1). De Schulten (1896) described the synthesis of darapskite crystals. Larsen (1921, p. 66) determined the optical properties of darapskite from Santa Catalina, about 15 miles northeast of Oficina Flor de Chile. Sabelli (1967) recently determined the crystal structure of darapskite from a synthetic crystal.

Features of the Nitrate Deposits

The nitrate deposits are in the Atacama Desert of northern Chile; they extend from about lat. 19°30′ S. to 26° S., a distance of nearly 700 kilometers (Fig. 1). Most are in a band less than 50 kilometers wide, between long. 69°30′ W. and 70° W. The region is characterized by the broad Central Valley bordered on the west by the relatively low Coastal Range, where few peaks are more than 2000 meters in altitude, and on the east by the Andes Mountains, where peaks extend to altitudes of 6000 meters or more. The most extensive nitrate deposits are along the broad, debris-covered slopes on the east side of the Coastal Range, but deposits also are found in closed basins within the Coastal Range and on gentle slopes and in broad valleys along the lower Andean front.

The nitrate deposits consist of caliche, generally not more than 2–3 meters in maximum thickness, in which diverse saline minerals (Table 1) occur as cement and impregnation in regolith and bedrock, and as associated high-purity veins. Cemented regolith is by far the most abundant type of nitrate ore and has been the source of most of the nitrate produced in Chile. It is relatively dense and surprisingly hard and tough. High-purity-nitrate-bearing veins in bedrock and in saline-cemented regolith are found throughout the nitrate region, and they were an important source of the sodium nitrate produced during the 19th century. The veins are excellent sources of mineralogical specimens and are still readily accessible in the many localities where they were mined underground.

The chemical composition and the mineralogy of the nitrate ore of Chile (Tables 1 and 2) are unique and indicate an unusual environment of formation. The unique suite of minerals results chiefly from the relatively high concentration of nitrate and iodate ions, which are sparse or absent in other saline deposits. The presence of these ions, together with chromate, CrO_4^{2-}, dicromate, $Cr_2O_7^{2-}$, and perchlorate, ClO_4^-, ions indicate an evironment of extremely high oxidation potential. The sources of these ions are not yet known. Some may have been supplied by normal weathering processes and atmospheric fallout, but others may have formed at the sites of the deposits themselves. Extreme aridity and paucity of microorganisms in the soil were probably important factors in the accumulation and preservation of the nitrate deposits.

Several minerals, in addition to those listed in Table 1, have been reported in the liter-

[1] Oficina, as used in the nitrate fields, refers to the site of the plant for treating nitrate ore.

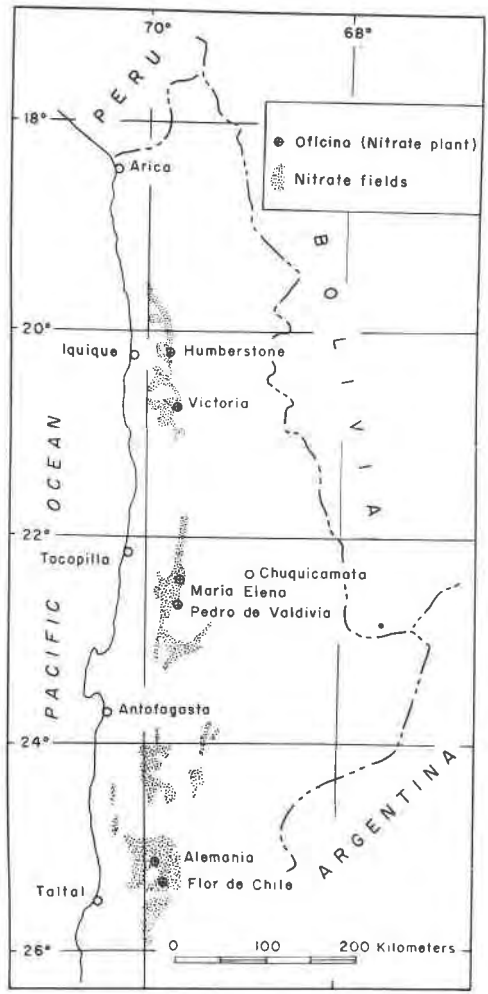

FIG. 1. Index map of northern Chile, showing location of nitrate fields.

ature but were not found in the material that we studied. Of these, only tarapacaite has been identified as a component of the nitrate ore (Brendler, 1923); the others either were misidentified or were reported on the basis of reconstituted chemical analyses. Our studies have revealed the presence of very small amounts of still other minerals, either minerals that heretofore have not been recognized as mineral species, or minerals for which published X-ray data are incorrect.

OCCURRENCE OF DARAPSKITE IN THE NITRATE DEPOSITS

Darapskite occurs in the nitrate ore as discrete crystals in cavities, as platy masses in veins, and as granular material admixed with other

TABLE 1. SALINE MINERALS OF THE NITRATE DEPOSITS OF CHILE IDENTIFIED IN THE PRESENT STUDY

Halite	$NaCl$	Bloedite	$Na_2Mg(SO_4)_2 \cdot 4H_2O$
Soda-niter	$NaNO_3$	Humberstonite	$K_3Na_7Mg_2(SO_4)_6(NO_3)_2 \cdot 6H_2O$
Niter	KNO_3	Ulexite	$NaCaB_5O_9 \cdot 8H_2O$
Darapskite	$Na_3(NO_3)(SO_4) \cdot H_2O$	Probertite	$NaCaB_5O_9 \cdot 5H_2O$
Thenardite	Na_2SO_4	Hydroboracite	$CaMgB_6O_{11} \cdot 6H_2O$
Anhydrite	$CaSO_4$	Ginorite	$Ca_2B_{14}O_{23} \cdot 8H_2O$
Gypsum	$CaSO_4 \cdot 2H_2O$	Kaliborite	$HKMg_2B_{12}O_{16}(OH)_{10} \cdot 4H_2O$
Bassanite	$2CaSO_4 \cdot H_2O$	Lautarite	$Ca(IO_3)_2$
Glauberite	$Na_2Ca(SO_4)_2$	Dietzeite	$Ca_2(IO_3)_2(CrO_4)$
Kieserite	$MgSO_4 \cdot H_2O$	Lopezite	$K_2(Cr_2O_7)$
Epsomite	$MgSO_4 \cdot 7H_2O$		

TABLE 2. CHEMICAL COMPOSITION OF WATER-SOLUBLE COMPONENTS IN NITRATE ORES OF NORTHERN CHILE (COMPOSITION IN WEIGHT PERCENT[a])

	1	2	3	4	5
NO_3^-	6.35	6.66	17.67	2.41	8.77
Cl^-	3.87	7.07	11.11	20.10	4.73
SO_4^{2-}	6.60	12.43	3.47	8.84	2.69
ClO_4^-	.035	.027	.57	1.0	.4
IO_3^-	.061	.068	.004	.03	.04
$B_4O_7^{2-}$	.36	.61	.07	.3	.2
Na^+[b]	6.2	8.9	13.8	14.6	6.4
K^+	.56	.61	.95	1.44	.28
Mg^{2+}	.15	.73	—	.71	—
Ca^{2+}	1.15	2.27	1.06	1.50	1.00
H_2O	1.74	1.08	1.87	2.76	4.87

1 Average grade of 5.97 million tons of nitrate ore treated at Oficina Pedro de Valdivia during 12-month period, July 1, 1935–June 30, 1936. Furnished by Anglo-Lautaro Nitrate Corp.

2 Average grade of 6.27 million tons of nitrate ore treated at Oficina María Elena, July 1, 1951–June 30, 1952. Furnished by Anglo-Lautaro Nitrate Corp.

3–5 Channel samples of selected parts of nitrate ore layer from two localities at Oficina Humberstone. Analyses by Empresa Salitrera Victoria of samples collected by Instituto de Investigaciones Geológicas of Chile.

[a] Recalculated in part by present authors from original analyses to facilitate comparison of analyses from different sources. Ions shown are the principal chemical components of nitrate ore, except for boron which exists largely as ulexite, $NaCaB_5O_9 \cdot 8H_2O$.

[b] Not determined in conventional analyses by nitrate companies of northern Chile. Calculated by present authors on basis of equivalent weights of reported components. Estimated to be within 1 percent of correct value.

saline minerals in veins, pods, and cementing material. Delicate tabular crystals, like those shown for synthetic darapskite in Figure 2, are by far the most abundant and widespread; prismatic crystals, as shown in Figure 3, were found at only a few localities. Veins of platy darapskite, found at a few localities only, consist of imperfect tabular crystals as much as 10 cm long and $\frac{1}{2}$ cm thick, oriented perpendicular to the walls of the vein. Granular darapskite is found associated with halite and soda-niter in veins, in encrustations in cavities, and in small pods or blebs as well as in finely disseminated saline cement.

Fig. 2. Cluster of thin tabular synthetic crystals of darapskite. Magnification 10×.

X-ray powder diffraction studies were indispensable to the identification of darapskite in the typical nitrate ore in which it is thoroughly admixed with other fine-grained white salts. These studies were facilitated by the extremely high sensitivity of the strongest line, $d = 10.30 \pm 1$ Å (Table 6). By means of an X-ray diffractometry study of known mixtures of soda-niter and darapskite it was determined that this line appeared in patterns taken of material containing as little as $\frac{1}{3}$ percent darapskite.

Physical and Optical Properties

The darapskite crystals utilized in this study came from three localities: near Oficina Victoria and near Oficina Alemania, both shown on Figure 1, and near Oficina Santa Lucia, which is not shown in Figure 1

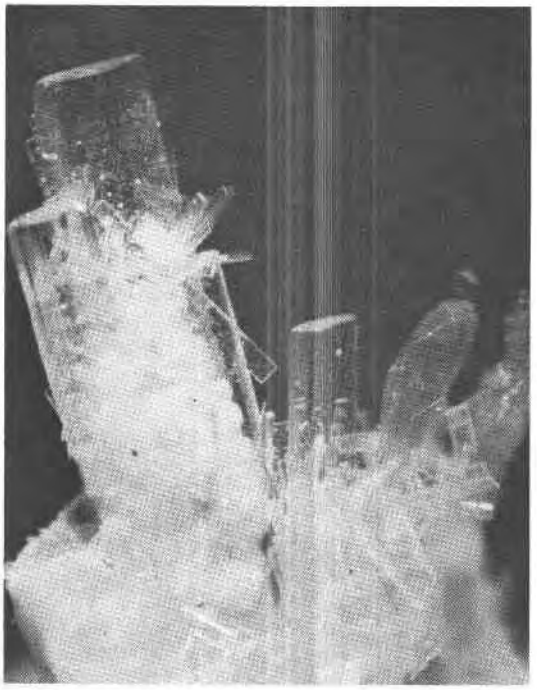

FIG. 3. Cluster of prismatic crystals of darapskite from nitrate fields at Oficina Alemania. Magnification 30×.

but which is about 25 kilometers southwest of Oficina Alemania. Tabular crystals from Oficina Santa Lucia occur as clusters of delicate, nearly square plates and long thin plates in cavities, appearing almost identical to the cluster of synthetic crystals shown in Figure 2. The nearly-square plates average about a millimeter long, $\frac{3}{4}$ mm wide, and $\frac{1}{10}$ mm thick; the long thin plates average 2 mm long, $\frac{1}{4}$–$\frac{1}{2}$ mm wide and less than $\frac{1}{10}$ mm thick. Similar crystals are found throughout the nitrate fields. Also common are larger individual thin darapskite plates in cavities; these plates are as much as 10 mm long, 8 mm wide, and $\frac{1}{10}$–$\frac{1}{2}$ mm thick. The largest single darapskite crystals, found at Oficina Victoria, are imperfect thick tabular crystals, 1–2 cm long and 3–4 mm thick. Prismatic crystals from Oficina Alemania (Fig. 3) average $1\frac{1}{2}$ mm long, $\frac{1}{2}$ mm wide, and $\frac{1}{4}$ mm thick. Long narrow tabular crystals are associated with the prismatic crystals, in part growing on them as shown in Figure 3.

The physical and optical properties of darapskite are tabulated in Table 3. The mineral is colorless and has a vitreous luster. Two directions of cleavage, {100} and {010}, were noted in the Chilean darapskite

TABLE 3. PHYSICAL AND OPTICAL PROPERTIES OF DARAPSKITE, $Na_3(NO_3)(SO_4)\cdot H_2O$

	Present Study		Larsen (1921)
	Oficina Alemania, Chile[a]	Synthetic Equivalent	Santa Catalina, Chile
Habit	Long prismatic c; also, thin tabular (100), elong. c	Square tabular (100), pseudo-tetragonal; also, tabular (100), elong. b	—
Color	Colorless, transparent to translucent	Colorless and transparent	Colorless and transparent
Hardness	$\sim 2\frac{1}{2}$	$\sim 2\frac{1}{2}$	—
Cleavage	{100} perf., {010} good	{100} perf., {010} very good	{100} and {010} perf.
Specific gravity	2.201±0.005, at 22°C	—	—
Optic sign	Biaxial negative (−)	Biaxial negative (−)	Biaxial negative (−)
Indices of refraction			
α	1.388±0.005	1.390±0.005	1.391±0.005
β	1.479±0.003 at 22°C	1.480±0.003 at 22°C	1.481±0.003
γ	1.486±0.003	1.486±0.003	1.486±0.003
Orientation			
X	b	b	b
Y	—	—	—
Z	+13°(±1°) to c	+13°(±1°) to c	12° to c
$2V$ (meas.)	small	small	27°±1°
$2V$ (calc.)	29°42′	27°36′	26°
Dispersion	$r>v$, strong	$r>v$, strong	$r>v$, rather strong
Twinning	Polysynthetic twinning; ∥{100}	Polysynthetic twinning; ∥{100}	Polysynthetic twinning; composition plane {100}
Mean meas. n	1.451	1.452	1.453[b]
Mean calc. n	1.449	1.449	1.449[b]

[a] Darapskite specimens from nitrate fields near the processing plant, the Oficina.
[b] Calculated by present authors.

as well as in its synthetic equivalent. Darapskite is brittle and has uneven fracture. It does not fluoresce in either long- or short-wave ultraviolet radiation. The specific gravity of darapskite from Oficina Victoria was determined (at 22°C) on the Berman microbalance with toluene as the immersion liquid; the average of four determinations on samples weighing from 20 to 22 mg is 2.201±0.005. This value is in good agreement with the value 2.197 determined (at 15°C) for synthetic crystals by de Schulten (1896).

The indices of refraction for darapskite from Oficinas Alemania and Santa Lucia (Table 3), and for the synthetic equivalent are in close agreement with those previously reported by Larsen (1921, p. 66) for crystals from Santa Catalina, Chile, and by Jarrell (1939) for crystals from Chuquicamata, Chile. Optical determinations were made with white light, and the immersion liquids were checked on the Abbe refractometer at the time the measurements were made. The liquid

($n=1.390$) used for the determination of the α index, a mixture of mineral oil and dimethylformamide, was prepared by Edward G. Williams of the U. S. Geological Survey.

Twinning is common in darapskite, with the twin plane parallel to $\{100\}$; re-entrant angles were noted on the edges of many darapskite crystals. Polysynthetic twinning was observed optically in sections cleaved normal to the *b*-axis; this type of twinning in darapskite was reported by Larsen (1921, p. 66) for crystals from Santa Catalina, Chile. Sabelli (1967, p. 874) reported that synthetic "crystals of darapskite show reticular pseudo-merohedral twinning, the twin axis being [001], with an obliquity of 1°26′ and an index of 2."

Crystallography

Single-crystal X-ray data. Precession photographs were obtained for a long prismatic crystal of darapskite from Oficina Alemania and also for a thin tabular synthetic crystal, using both zirconium-filtered molybdenum radiation ($\lambda MoK\alpha=0.71069$ Å) and nickel-filtered copper radiation ($\lambda CuK\alpha=1.5418$ Å). The diffraction data show monoclinic symmetry that is compatible with space groups $P2_1$ and $P2_1/m$. The morphology of the crystals supports $P2_1/m$ as the space group for darapskite; the recent crystal-structure determination by Sabelli (1967) confirms $P2_1/m$ as the correct space group.

Preliminary cell parameters were obtained from measurements of *h*0*l*, *hk*0, and 0*kl* precession photographs of both crystals. These were used together with the observed powder diffraction data for both types of crystals to obtain the refined cell data that are compared in Table 4 with those recently reported by Sabelli (1967). The specific gravity calculated from the cell data for darapskite from Oficina Alemania and for synthetic darapskite are in excellent agreement with measured values (Table 4).

Morphology. Crystals of darapskite used in the morphological study are from cavities in specimens of nitrate ore from Oficina Alemania and Oficina Santa Lucia. A specimen from Oficina Alemania contained two types of darapskite crystals, as shown in Figure 3: 1) thick translucent prismatic crystals and 2) very thin transparent tabular crystals that are long and narrow; both types of crystals are elongated *c* and flattened on (100). Crystals from Oficina Santa Lucia are mainly thick, square to slightly rectangular tablets, but long narrow tablets also are present; both types are flattened on (100). The long narrow tabular crystals from this locality are elongated in the *b*-direction, in contrast to similar crystals from Oficina Alemania which are elongated in the *c*-direction.

TABLE 4. CRYSTALLOGRAPHIC DATA FOR DARAPSKITE, $Na_3(NO_3)(SO_4)\cdot H_2O$, AND ITS SYNTHETIC EQUIVALENT

	Present Study[a]		Sabelli (1967)
	Darapskite from near Oficina Alemania, Chile	Synthetic Equivalent	Synthetic Equivalent
Space Group	$P2_1/m$	$P2_1/m$	$P2_1/m$
a (Å)	10.564±0.002	10.571±0.003	10.564±0.001
b (Å)	6.913±0.001	6.917±0.002	6.911±0.003
c (Å)	5.1890±0.0009	5.1891±0.0010	5.194±0.002
β	102°47.8′±0.8′	102°46.6′±1.1′	102.78°±0.02°
$a:b:c$	1.5281:1:0.7506	1.5283:1:0.7502	1.5286:1:0.7516
Cell Volume (Å^3)	369.5	370.0	[369.8][b]
Z	2	2	2
Specific Gravity			
ρ calc.	2.202	2.199	2.16 [2.201][b]
ρ meas.	2.201±0.005,at 22°C	2.197, at 15°C[c]	—

[a] Unit-cell constants refined using powder diffraction data of Table 6, and the computer program of Evans *et al.* (1963).

[b] Calculated by the present authors from data of Sabelli (1967).

[c] From de Schulten (1896), on synthetic crystals.

Crystals of synthetic darapskite, like those of darapskite from Oficina Santa Lucia, are square tabular, but extremely thin. Darapskite crystals from Oficina Alemania are attached to the walls of the cavities at one end of the c-axis; those from Oficina Santa Lucia, at one end of the b-axis. The synthetic crystals form rosette-like aggregates of tabular crystals that are oriented so that they are joined together at one end of the b-axis.

Many naturally occurring and synthetic crystals were measured on the reflecting goniometer. On every crystal $a\{100\}$ is the dominant form. The same forms, measured and identified on the darapskite crystals from the two Chilean localities, also were found on crystals synthesized in this study; these are listed and compared in Table 5 with those described by Osann (1894) and by de Schulten (1896). Only a few of the many synthetic crystals examined had the form $q\{011\}$. None of the general forms *hkl* reported by Osann (1894) was found on any of the crystals that we examined.

X-ray powder diffraction data. As far as we know, X-ray powder diffraction data for neither darapskite nor its synthetic equivalent have ever been published. Powder data for darapskite from Oficina Alemania and

synthetic darapskite are listed in Table 6. Patterns of darapskite from Oficina Santa Lucia and Oficina Victoria also were made for purposes of identification and comparison. In addition, a pattern was made of fragments of darapskite from Santa Catalina, Chile (Col. W. Roebling's specimen), the remainder of the original material used by Larsen (1921, p. 66) for optical determinations.

X-ray powder patterns of darapskite were taken with several different types of spindle-mounts (ball mount, segmented spindle, and glass capillary filled with a darapskite-glass mixture) to check for preferred orientation due to the perfect (100) cleavage. No preferred orientation effects were detected, despite the different types of mounts used.

Chemical Properties

Composition. The chemical composition of darapskite (Dietze, 1891, p. 445) from Oficina Lautaro agrees well with the calculated composition of darapskite:

	Darapskite Calculated Composition $Na_3(NO_3)(SO_4)\cdot H_2O$ (Weight Percent)	Darapskite Oficina Lautaro Dietze (1891) (Weight Percent)
Na_2O	37.94	38.27
N_2O_5	22.04	22.26
SO_3	32.67	32.88
H_2O	7.35	7.30
Total	100.00	100.71

Solubility. Darapskite is readily soluble in water but only slightly soluble in acetone and alcohol. In alcohol, clear crystals first turn white due to desiccation, and then $NaNO_3$ is dissolved slowly, leaving a residue of Na_2SO_4. Crystals remain clear in acetone but are leached slowly, $NaNO_3$ going into solution and Na_2SO_4 remaining as a residue.

Synthesis. Crystals of darapskite were grown in the laboratory to provide material for comparison with darapskite from Chilean localities. The procedure followed for synthesizing darapskite was similar to that outlined in detail by de Schulten (1896). Anhydrous sodium sulfate (22.044 g) was dissolved in 128 cc of boiling water, and to this solution 80 g of sodium nitrate gradually was added, while the solution was constantly stirred. This solution then was filtered, and allowed to cool to room temperature (22°C) in an open vessel. The darapskite crystallized as the solution cooled, forming aggregates of delicate platy crystals like those shown in Figure 2. The crystals were removed and dried between filter paper. About 7 g of darapskite were obtained in this manner.

De Schulten (1896, p. 163–164) showed that Marignac (1857) synthesized darapskite long before the mineral was discovered and described by Dietze (1891). By evaporating a solution of sodium sulfate and sodium nitrate Marignac obtained tabular crystals to which, on the basis of chemical analysis, he assigned the formula $2NaNO_3\cdot 2Na_2SO_4\cdot 3H_2O$.

TABLE 5. FORMS OBSERVED ON DARAPSKITE CRYSTALS

Forms	Present Study (1)	(2)	(3)	Osann (1894) (4)	de Schulten (1896) (5)
c 001	×	×	×	×	×
b 010	×	×	×	×	×
a 100	×	×	×	×	×
m 110	×	×	×	×	×
q 011			×	×	
r 101	×	×	×	×	×
e 302				×	×
n $\bar{1}01$	×	×	×	×	
d $\bar{2}01$	×	×	×	×	×
o 111				×	
s $\bar{1}11$				×	
v 121				×	

(1) Oficina Santa Lucia, Chile.
(2) Oficina Alemania, Chile.
(3) Synthetic equivalent.
(4) Oficina Lautaro, Chile.
(5) Synthetic equivalent.

Except for the slight excess of H_2O, probably due to analytical error, this formula ($=2[Na_3(NO_3)(SO_4)\cdot 1\frac{1}{2}H_2O]$ is the same as that of darapskite.

Thermogravimetric characteristics. The thermogravimetric curves shown in Figure 4 were made and interpreted by Frederick Simon of the U. S. Geological Survey. The darapskite curve was made of material from Oficina Victoria. The other curves are for the reagent-grade chemicals, $NaNO_3$ and Na_2SO_4. Runs were made on 50 mg samples with a thermogravimetric balance which automatically records the weight of the sample as the temperature rises to a maximum of 1000°C. The curve for darapskite shows a loss of water between the temperatures of 85°C and 125°C, amounting to a 7.3 percent weight loss, which is approximately the water content of this mineral. No loss in weight takes place between 125°C and 300°C, but between 300°C and about 600°C there is a gradual loss of weight, amounting to about 2 percent. This loss probably results from incipient decomposition of $NaNO_3$. A major weight loss between 600° and 800°C (about 15 percent) represents complete decomposition of the $NaNO_3$, during which NO_2 is given off; a residue consisting of Na_2O and Na_2SO_4 remains. Additional weight loss to 1000°C results from loss of Na_2O as a sublimate.

Several X-ray powder diffraction patterns were made of darapskite

TABLE 6. X-RAY POWDER DATA FOR DARAPSKITE, $Na_3(NO_3)(SO_4)\cdot H_2O$

hkl	Oficina Alemania, Chile			Synthetic Equivalent		hkl	Oficina Alemania, Chile			Synthetic Equivalent	
	Calculated[a]	Measured[b]		Measured[c]			Calculated[a]	Measured[b]		Measured[c]	
	d (Å)	d (Å)	I[d]	d (Å)	I[d]		d (Å)	d (Å)	I[d]	d (Å)	I[d]
100	10.302	10.29	100	10.32	100	$\bar{1}22$	2.076				
110	5.740	5.74	2	5.74	2	$\bar{5}01$	2.075				
200	5.151					321	2.071	2.070	13	2.072	11
001	5.060	5.06	3	5.05	2	420	2.065				
$\bar{1}01$	5.001					500	2.060				
101	4.190					$\bar{4}02$	2.046				
210	4.130	4.13	25	4.13	21	$\bar{4}21$	2.043				
$\bar{2}01$	4.091					022	2.042	2.040	2	2.043	3
011	4.083					$\bar{2}22$	2.026				
$\bar{1}11$	4.052	4.05	2	4.06	2	411	2.021				
111	3.583	3.585	13	3.585	11	131	2.019				
$\bar{2}11$	3.521	3.522	25	3.525	18	$\bar{2}31$	2.008	2.011	4	2.013	4
020	3.456	3.456	35	3.459	35	212	2.005				
300	3.434					$\bar{5}11$	1.9879	1.9885	1		
120	3.277					510	1.9745				
201	3.266	3.266	18	3.271	18	$\bar{4}12$	1.9615	1.9625	1	1.9613	2
$\bar{3}01$	3.188	3.188	18	3.190	11	122	1.9377	1.9372	11	1.9380	9
310	3.075	3.077	2	3.079	3	330	1.9134				
211	2.953	2.953	7	2.955	4	$\bar{3}22$	1.9114	1.9106	11	1.9120	3
$\bar{3}11$	2.895					231	1.8829				
220	2.870			2.871[e]	30	$\bar{3}31$	1.8676	1.8671	2		
021	2.854	2.865	35	2.856[e]	30	302	1.8506				
$\bar{1}21$	2.844					$\bar{5}02$	1.8054	1.8052	2		
121	2.666	2.666	9	2.667	7	421	1.8033				
$\bar{2}21$	2.640					501	1.7758	1.7737	13	1.7737	11B
$\bar{1}02$	2.594	2.594	30	2.594	30			1.7480	3	1.7481	2
301	2.588							1.7288	9	1.7284	9
400	2.575							1.7046	3	1.7053	2
$\bar{4}01$	2.533	2.534	7	2.534	7			1.6731	1	1.6732	2
002	2.530							1.6293	2D	1.6294	2D
$\bar{2}02$	2.501	2.502	1					1.6067	3	1.6067	2
320	2.436	2.436	13	2.438	9					1.5954	2
$\bar{1}12$	2.428							1.5804	2	1.5804	1
311	2.423	2.423	2	2.421	2			1.5400	1D	1.5400	1
410	2.413							1.5172	1	1.5172	1
$\bar{4}11$	2.379	2.378	3	2.378	2			1.5030	2	1.5024	4
012	2.376							1.4713	3	1.4720	3
221	2.374							1.4490	3	1.4497	2
$\bar{2}12$	2.352							1.4386	4	1.4389	3
$\bar{3}21$	2.344							1.4256	1	1.4256	1D
102	2.340	2.342	4	2.341	3			1.3932	1		
$\bar{3}02$	2.294	2.292	1					1.3789	1	1.3789	2
130	2.249	2.250	6	2.251	4			1.3517	2	1.3517	3
112	2.216	2.213	1	2.215	2			1.3365	2	1.3359	1
$\bar{3}12$	2.177	2.176	4	2.177	4			1.3133	2	1.3128	1
401	2.114							1.2943	4	1.2948	2
230	2.103							Plus 20 additional lines with I≤3.			
031	2.097	2.096	2	2.100	2						
202	2.095										
$\bar{1}31$	2.093										

[a] Calculated from these unit-cell parameters: $a=10.564$ Å, $b=6.913$ Å, $c=5.1890$ Å, $\beta=102°47.8'$, with space group $P2_1/m$. All possible calculated spacings are given to $d\geq 1.7700$ Å.

[b] Camera diameter, 114.59 mm. Mn-filtered Fe radiation ($\lambda FeK\alpha=1.9373$ Å). Wilson-type pattern. Film shrinkage negligible. Lower limit measurable for 2θ: approximately 6.0° (18.5 Å).

[c] Camera diameter, 114.59 mm. Mn-filtered Fe radiation ($\lambda FeK\alpha=1.9373$ Å). Internal standard, CaF_2. Wilson-type pattern. Film shrinkage negligible. Lower limit measurable for 2θ: approximately 6.0° (18.5 Å).

[d] Intensities estimated visually by direct comparison with a calibrated intensity film strip of successive step-line exposures related to each other by a factor of $\sqrt{2}$. B = broad; D = diffuse.

[e] Measurements obtained from a film taken in V-filtered Cr radiation ($\lambda CrK\alpha=2.2909$ Å).

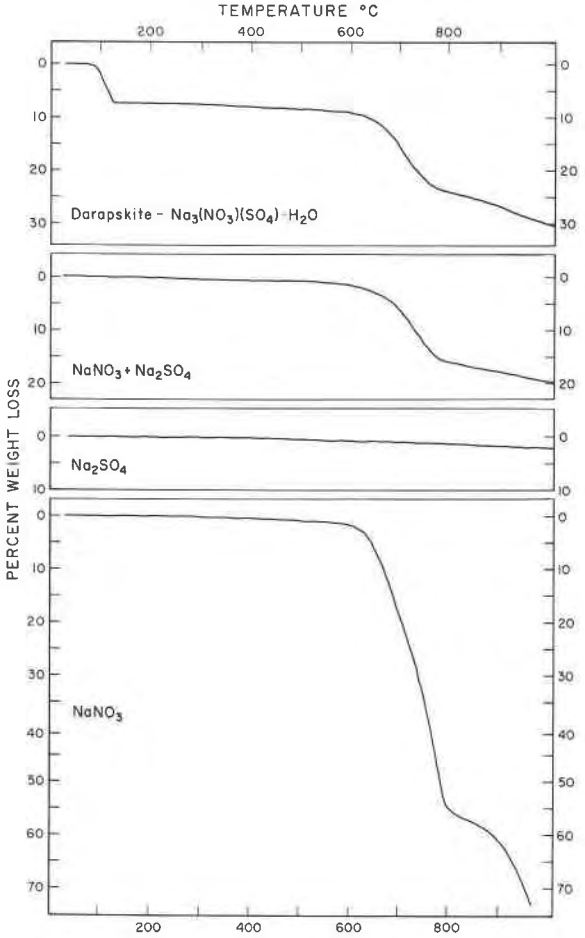

FIG. 4. Thermogravimetric curve for darapskite compared with curves for $NaNO_3$, Na_2SO_4, and an equimolar mixture of $NaNO_3$ and Na_2SO_4.

that had been heated to 110°–125°C to drive off the water. These patterns showed the residue to consist of hexagonal $NaNO_3$, corresponding to soda-niter, and hexagonal Na_2SO_4, corresponding to meta-thenardite, the high-temperature form of thenardite referred to as Type I (Bird, 1958).

Infrared characteristics. Infrared spectra of darapskite (Fig. 5) from the nitrate fields at Oficina Victoria were made under the direction of Irving A. Berger of the U. S. Geological Survey, who also aided in their in-

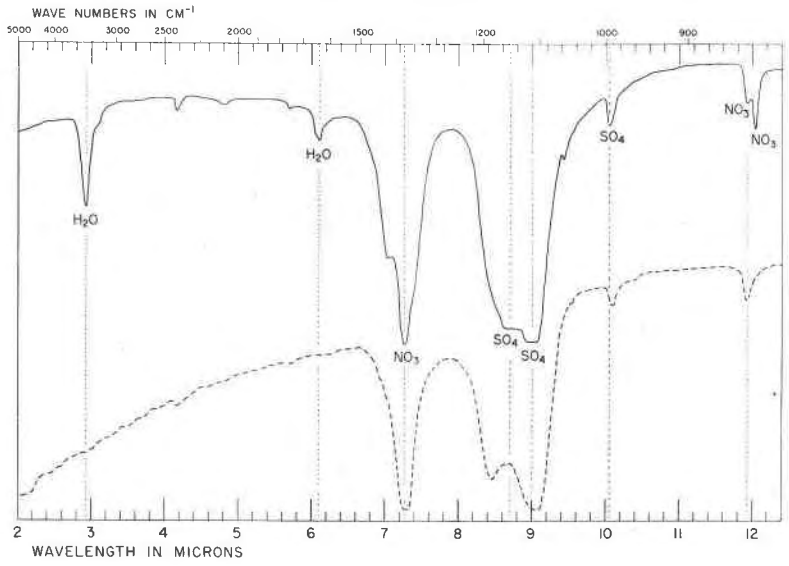

FIG. 5. Infrared spectra of darapskite: solid curve is spectrum at room temperature (about 22°C); dashed curve is spectrum at 110°C.

terpretation (Table 7). The instrument used was a Perkin-Elmer model 21 spectrophotometer with NaCl optics. The spectrum shown by the solid curve (Fig. 5) was made of a pellet consisting of 1 mg of darapskite in 300 mg of KBr maintained at room temperature and analyzed against a reference 300 mg pellet of KBr, also at room temperature. The spectrum shown by the dashed curve is of the same pellet (after slowly being heated to 110°C to drive off the water) analyzed at 110°C against a reference 300 mg KBr pellet maintained at 110°C. Therefore, the first curve is of the mineral darapskite, whereas the second curve is of a mixture of anhydrous $NaNO_3$ and Na_2SO_4.

Table 7 shows the absorptions corresponding to the fundamental modes of vibration (ν_1, ν_2) that are active for NO_3^- and SO_4^{2-} in darapskite and related compounds. According to Adler (1965), the vibrational modes for "lattice water" are near 3 μm ($\nu_s = \nu_1$ and ν_3) and 6 μm ($\nu_b = \nu_2$). As can be seen in Table 7, the absorptions corresponding to both NO_3^- and SO_4^{2-} peaks in the curve of the heated "darapskite" are similar to those for natural darapskite. However, the infrared spectrum of the unheated darapskite shows a weak absorption at 13.64 μm (not shown in Table 7 and Fig. 5), which may correspond to the ν_4 absorption of NO_3^- reported by Weir and Lippincott (1961). This spectrum also shows a second ν_2 absorption at 12.04 μm. The spectrum of heated

TABLE 7. ABSORPTION WAVELENGTHS FOR INFRARED SPECTRA SHOWN IN FIGURE 5 COMPARED WITH SPECTRA OF $NaNO_3$ AND THENARDITE

Samples	H_2O		NO_3^-			SO_4^{2-}		
	ν_a	ν_b	ν_2		ν_3	ν_1	ν_2	
Darapskite (spectrum at 22°C)[b]	2.92[a] (3430)	6.10 (1640)	12.04 (830)	11.93 (838)	7.27 (1377)	10.05 (995)	9.00 (1112)	8.70 (1150)
Darapskite (spectrum at 110°C)[c]				11.92 (838)	7.28 (1375)	10.10 (990)	9.06 (1103)	8.46 (1182)
$NaNO_3$[d]				11.98 (835)	7.30 (1370)			
Thenardite[e]						10.09 (991)	8.96 (1116)	

[a] Wavelength in μm; number within parenthesis is wavenumber in cm^{-1}.
[b] Pellet of 1 mg of darapskite in 300 mg of KBr.
[c] Same pellet as was used for the darapskite spectrum at 22°C.
[d] Reagent grade $NaNO_3$.
[e] Spectrum of Adler and Kerr (1965, p. 144).

"darapskite" shows neither of these peaks; it does, however, show an absorption at 8.46 μm (corresponding to SO_4), which is not present in the spectrum of thenardite.

PHASE RELATIONS

Because of their importance in the extraction of sodium nitrate from the Chilean nitrate ores, the phase relations of darapskite and other saline components of the ores have been studied extensively. The basic process of the nitrate plant is one of selective leaching of crushed nitrate ore with a heated brine that is then cooled to crystallize sodium nitrate. The brine is recycled in the process, and solubility data are essential for controlling its composition to assure the most efficient extraction of nitrate from the ore and to crystallize a pure sodium nitrate product. Of particular importance is control to inhibit crystallization of darapskite as a contaminant in the final product, a very serious problem with some of the high sulfate ores.

Foote (1925) reported that darapskite was stable over the widest range of concentrations in the system $NaNO_3$–Na_2SO_4–H_2O at 24.5°C and that above and below this temperature the range diminishes. The lowest

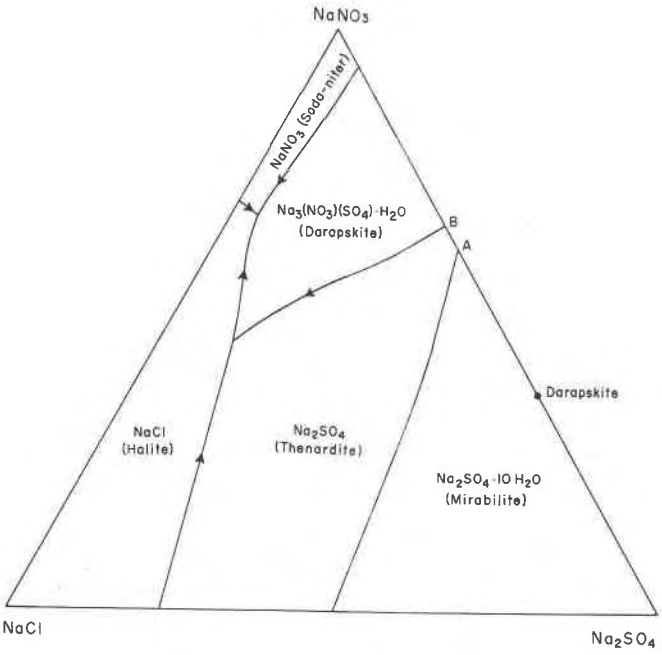

FIG. 6. Jänecke diagram of the system $NaNO_3$–NaCl–Na_2SO_4–H_2O, at 25°C. Plotted in weight percent from solubility data of Chretien (1926*b*, p. 406).

temperature at which darapskite formed in this system was found to be 13.5°C, and the highest temperature, obtained by extrapolation of the solubility data, was estimated to be near 50°C. Chretien (1926*a*, p. 544) concluded from his study of this system that darapskite formed in the temperature range 13°–74°C. Another study by Chretien (1926*b*) showed that in the system $NaNO_3$–NaCl–Na_2SO_4–H_2O, darapskite forms at temperatures ranging from 7.2°C to 71.5°C. The presence of NaCl apparently causes a lowering of the temperature range of stability of darapskite.

The phase relations of the principal saline constituents of nitrate ore ($NaNO_3$, NaCl, and Na_2SO_4) are presented in Figure 6 for the temperature of 25°C, which probably is within the range of the temperature of formation of the nitrate deposits. The diagram is a Jänecke diagram which does not show the component H_2O and therefore indicates the ratios of the saline components in an aqueous solution rather than their concentration. Any point in the diagram represents 100 percent (by weight) of one or more of the components shown at the corners. As can be seen in Figure 6, darapskite has a composition that lies outside the field

in which it precipitates; that is, it shows incongruent solubility, crystallizing from a solution in which the relative amounts of its component ions (Na^-, SO_4^{2-}, NO_3^-) differ from those in the mineral.

The phase diagram helps to explain the paucity or absence of thenardite in a typical nitrate ore that contains abundant soda-niter and less abundant, but widespread, darapskite. The thenardite and soda-niter fields are separated by the darapskite field; therefore, thenardite and soda-niter could not co-exist if equilibrium conditions were maintained during crystallization at this temperature. Chretien (1926*b*) has shown that in this system mirabilite and soda-niter can coexist only at temperatures below 13°C, and thenardite and soda-niter only above 68.5°C.

ACKNOWLEDGMENTS

The many people who have aided our investigations are too numerous to mention individually. We do, however, wish to express our appreciation for aid and hospitality to the nitrate companies operating in Chile in the 1960's: Anglo-Lautaro Nitrate Corporation, owner of Oficinas María Elena and Pedro de Valdivia; Compañía Salitrera Pedro Perfetti, owner of Oficina Flor de Chile; Compañia Salitrera Iquique, owner of Oficina Alemania; and Empresa Salitrera Victoria, owner of Oficina Victoria. These companies furnished much information about the physical and chemical characteristics of nitrate ores and made special chemical analyses of some of our nitrate-ore samples.

We wish also to thank our colleagues of the U. S. Geological Survey for the various laboratory determinations: Irving A. Breger, for the infrared spectra; William B. Crandell, for a semiquantitative spectrographic analysis; Judith Konnert, for refinement of the X-ray diffraction powder data; Frederick Simon, for the thermogravimetric determinations; and Edward G. Williams, for preparation of the special index liquid that was required for determination of the refractive indices of darapskite.

REFERENCES

ADLER, H. H. (1965) Examination of mass-radius effects, hydrogen bonding and ν_b splitting in infrared spectra of Zr-Hf homologs. *Amer. Mineral.* **50,** 1553–1562.

——— AND P. F. KERR (1965) Variations in infrared spectra, molecular symmetry and site symmetry of sulfate minerals. *Amer. Mineral.* **50,** 132–147.

BIRD, R. J. (1958) Polymorphic transitions in anhydrous sodium sulfate. *Nature,* **182,** 1797–1798.

BRENDLER, W. (1923) Uber tarapacait. *Z. Kristallogr.* **58,** 445–447.

CHRETIEN, ANDRE (1926*a*) Estudio del sistema ternario, agua-sulfato de sodio-nitrato de sodio. *Caliche,* **7,** 439–453, 500–503, and 542–545.

——— (1926*b*) Sistema cuaternario: agua-nitrato de sodio-cloruro de sodio-sulfato de sodio entre 100° y 0°. *Caliche,* **8,** 390–408.

CLARIDGE, G. G. C. AND I. B. CAMPBELL (1968) Origin of nitrate deposits. *Nature,* **17,** 428–430.

DIETZE, AUGUST (1891) Einige neue chilenische Mineralien. *Z. Kristallogr.* **19,** 443–451.

EVANS, H. T., JR., D. E. APPLEMAN, AND D. S. HANDWERKER (1963) The least-squares refinement of crystal unit cells with powder diffraction by an automatic computer indexing method [abstr.]. *Amer. Crystallogr. Assoc., Annu. Meet., Program,* **1963,** 42–43.

FOOTE, H. W. (1925) The system sodium nitrate-sodium sulphate-water, and the minerals darapskite and nitroglauberite. *Amer. J. Sci.* **9,** 441–447.

JARRELL, O. W. (1939) Marshite and other minerals from Chuquicamata, Chile. *Amer. Mineral,* **24,** 629–635.

LARSEN, ESPER S. (1921) The microscopic determination of the non-opaque minerals. *U. S. Geol. Surv. Bull.* **679,** 294 p.

MARIGNAC, C. (1857) Sur les formes cristallines et la composition chimique de divers sels. *Ann. Mines,* ser. 5, **12,** 1–74.

MROSE, M. E., AND G. E. ERICKSEN (1970) Mineralogical studies of the nitrate deposits of Chile (I): The identity of nitroglauberite with darapskite. *Amer. Mineral.* **55,** 776–783.

OSANN, A. (1894) Krystallographische Untersuchung einiger neuer chilenischer Mineralien. *Z. Kristallogr.* **23,** 584–589.

PALACHE, CHARLES, HARRY BERMAN AND CLIFFORD FRONDEL (1951) *The System of Mineralogy . . . of Dana, 7th ed., Vol. 2.* John Wiley and Sons, Inc., New York, 309–311.

SABELLI, CESARE (1967) La struttura della darapskite. *Atti Accad. Naz. Lincei, Rend. Cl. Sci. Fis. Mat. Nat.* **42,** 874–887.

DE SCHULTEN, A. (1896) Sur la reproduction artificielle de la darapskite. *Bull. Soc. Fr. Mineral. Cristallogr.* **19,** 161–164.

WEIR, C. E., AND E. R. LIPPINCOTT (1961) Infrared studies of aragonite, calcite, and vaterite type structures in the borates, carbonates, and nitrates. *J. Res. Nat. Bur. Stand. A* **65,** 173–183.

Manuscript received, February 4, 1970; accepted for publication, March 31, 1970